Proceedings of the 28th IEEE
EMBS Annual International Conference
New York City, USA, Aug 30-Sept 3, 2006

Calculation of Wall Shear Stress in Left Coronary Artery Bifurcation for Pulsatile Flow Using Two-Dimensional Computational Fluid Dynamics

Sahid Smith[1], Shawn Austin[1], G. Dale Wesson[*1,2], and Carl A. Moore
[1] Florida A&M University, Department of Chemical Engineering and Biomedical Engineering, Tallahassee, FL 32310
[2] Florida A&M University, Biological and Agricultural Systems Engineering Program, Tallahassee, FL 32307
[3] Florida A&M University, Department of Mechanical Engineering, Tallahassee, FL 32310

Abstract- **The onset of coronary heart disease may be governed by distribution and magnitude of hemodynamic shear stress in the coronary arteries. This study numerically examines pulsatile blood flow through the left coronary artery system. A triphasic waveform is employed to simulate pulsating flow. Five non-Newtonian models, as well as the usual Newtonian model, are used to describe the viscous shear-thinning behavior of blood.**

It is concluded that when using computational fluid dynamics (CFD) to numerically investigate blood velocity profiles within small arteries, such the coronary artery system examined in this work, great care should be taken in choosing a blood viscosity model. It is suggested hat the Generalized Power Law model be the viscous shear thinning model of choice. When using CFD to investigate only patterns of wall shear stresses, the model selection is not as crucial and the simple Newtonian model will suffice but when the magnitude of WSS is of great importance, as in the case of the determining the development of coronary artery disease, the model selection is key.

I. INTRODUCTION

The distribution of wall shear stress (WSS) in the coronary arteries is believed to be a significant determinant of the commencement of coronary heart disease [1-4]. Numerical modeling and computational fluid dynamics (CFD) have become reliable methods of predicting flow characteristics, and have been employed in investigations of several cardiovascular systems. Several researchers have successfully employed CFD to simulated blood flow through various vessels of the cardiovascular system. Many have assumed blood to behave as an incompressible Newtonian fluid experiencing steady[5] and pulsatile flow[6-8]. Johnston et al.[9] compared the results of various non-Newtonian models for steady flow. Rolf and Tenti[10] investigated the role of the Wormersley number in determining whether blood should be modeled as a Newtonian or non-Newtonian fluid. The current study numerically simulates unsteady pulsatile blood flow through an idealized anatomically proportioned two-dimensional left coronary artery (LCA) system. Five non-Newtonian blood models, which include the Power Law, Walburn-Schneck, Carreau, Casson, and Generalized Power Law models, and a Newtonian model are compared in the simulation of blood flow in the left coronary artery system.

II. METHODS

A. Geometry

Blood flow in the human left coronary artery (LCA) system is examined in this investigation. The LCA system is comprised of three blood vessels; the left main (LM), left anterior descending (LAD), and the left circumflex (LCX) arteries. The flow geometry was constructed from arterial data presented by He and Ku [7]. The data represents an idealized model of the left coronary artery system that was developed from average dimensions of LM, LAD, and LCX from 35 post-mortem casts of normal human coronary artery trees with root of the aorta. The average diameters of the LM, LAD, and LCX are 4.0mm, 3.4mm and 3.0 mm, respectively. A two dimensional representation of the LCA system is shown in Fig. 1.

The major flow characteristics directly related to the localization of atherosclerotic plaques are low fluid velocity and the resultant low WSS [11]. In this investigation, it is assumed that the slight curvature of the coronary artery can be ignored when investigating the location and magnitude of this WSS. Future 3-D investigations will evaluate the validity of this hypothesis. Therefore, the following geometric assumptions are adopted:

1. The flow domain is two- dimensional.
2. The curvature of the LCA system is neglected.
3. The LM, LCX, and LAD are composed of straight smooth rigid walls.

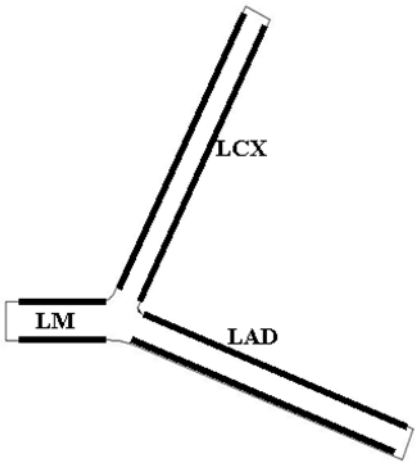

Fig. 1. Two-Dimensional representation of the LCA system. The figure shows the three blood vessels (LM, LAD, and LCX) that comprises the LCA system.

B. Governing Equations and Boundary Conditions

It is assumed that blood may be represented by an incompressible fluid governed by the continuity equation

$$\nabla \cdot \mathbf{u} = 0 \quad (1)$$

and the Navier-Stokes equations

$$\rho \frac{D\mathbf{u}}{Dt} = -\nabla P + \mu \nabla^2 \mathbf{u} \quad (2)$$

where $\mathbf{u}$ is the velocity vector, P is pressure, t is time, μ is viscosity, and ρ is density. Writing the Navier-Stokes equations in the form seen in (2) allows the various non-Newtonian models described in Table 1 to be implemented. In this work, the density of blood is assigned a value of 1050 kg/m^3. These assumptions have been previously shown to be reasonable for arterial hemodynamics by several investigators [12].

The governing equations are solved numerically with Fluent 6.2© (Fluent Inc., Lebanon NH, USA), a commercially available computational fluid dynamics software package. A finite volume mesh is created based on the arterial data obtained previously published by He and Ku [7]. The two-dimensional mesh consisted of 3196 cells and 1775 nodes. The finite volume mesh was constructed using the grid generation package Gambit (Fluent Inc., Lebanon NH, USA).

To solve the governing equations numerically, a set of boundary conditions is required.

The following boundary conditions were applied to the governing equations:

1. No slip, i.e. $\mathbf{u} = 0$, at all arterial walls
2. The velocity profile entering the flow domain was assumed to be uniform. This inlet velocity was a function of time and was approximated as the triphasic waveform.
3. Volumetric flow splits of 0.5928 for the LAD and 0.4072 for the LCX were assumed. (Note: the volumetric flow split of 0.5928 for the LAD means 59.28 % of the volumetric flow from LM proceeds down the LAD.) Flow division between the LAD and the LCX was based on the assumption that the branching arteries sustained the same mean shear rate.

A time step equivalent to 1/100th of the cardiac cycle was employed. A total of 6081 iterations were performed and required 0.044 s to compute per iteration. The computational simulations were performed on a Windows-based Dell Precision 670 Workstation 2000 with dual processors running at 3.6 Ghz.

III. RESULTS & CONCLUSIONS

Atherogenesis preferentially involves the outer walls of vessel bifurcations and points of blood flow recirculation and stasis [4, 7, 11]. In these geometrically predisposed locations, the wall shear stress is significantly lower in magnitude and exhibits directional changes [4, 7, 13, 14]. Flow separation is also a common feature in these locations. Direct measurements and flow models of these susceptible regions have revealed WSS on the order of ±0.4 Pa; and in regions where atheromatous legions are not commonly found WSS were greater than 1.0 Pa [14]. These associations with WSS suggest that elevated levels (greater than 1.0 Pa) of WSS might shield against atherosclerosis. Fig. 2 displays the range of wall shear stress magnitudes and their implications encountered in veins and arteries.

The findings of this study serve three major functions. First, they demonstrate the complex nature of the WSS that is generated from pulsatile flow in the left coronary artery system. Second, the findings of this investigation illustrate how the choice of a rheological model affects WSS magnitude and distribution predictions. Third, the results can be used in conjunction with a general knowledge of the flow characteristics to predict the velocity distribution within the left coronary artery system.

A. Rheological Models

One aspect of this study involved considering the effect of several rheological models on the WSS distribution in the coronary arteries. In total, six rheological models (five non-Newtonian and one Newtonian) were considered and compared with viscometric data [15]. The rheological models, their respective parameters, and modifications were summarized in Table 1. Comparisons of the viscosity predicted by the various models revealed the Newtonian, Casson, Walburn-Schneck, Power Law, Carreau, and Generalized Power Law models resulted in average percent errors of 76.22%, 51.16%, 46.51%, 30.61%, 12.19%, and 3.79%, respectively when compared with the experimental data presented by Chien [15]. The

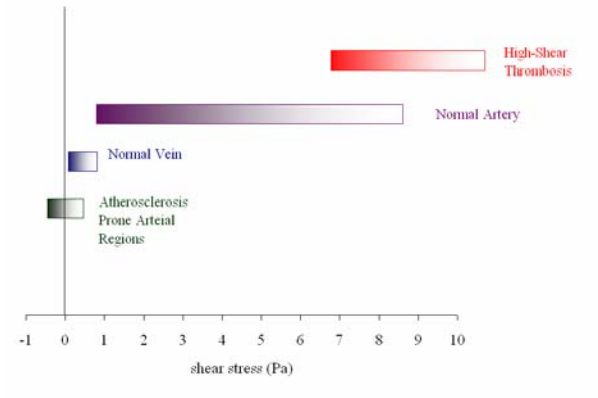

Fig. 2. The range of wall shear stress magnitudes. The diagram illustrates the range of shear stress magnitudes encountered in veins, arteries, and in low-shear and high-shear pathologic states.

Generalized Power Law model is the model of choice for CFD predictions of the WSS of pulsatile flow in the left coronary artery because of its low percent error.

B. WSS Distributions

This study has placed an emphasis on the distribution of the wall shear stress within the LCA. It is generally believed that the WSS is an important hemodynamic variable in the onset of atherosclerotic lesions. The results obtained in this study reflect the complex nature of the WSS patterns in the left coronary artery system.

One of the most evident observances from the results was the magnitude of the WSS was always greater in the interior of the LM (ranging from 0.75 Pa to 7.0 Pa during the cardiac cycle), than the interior of the LAD or LCX (ranging from 0.47 Pa to 3.2 Pa in the LAD and 0.20 Pa to 1.4 Pa in the LCX during the cardiac cycle). This would suggest that LAD and LCX are more susceptible than the LM to the development of the atherosclerotic legions that lead the coronary artery disease. It is generally accepted that atherosclerotic legions develop in regions within the coronary artery where the WSS is low and oscillating [3, 7, 13, 16]; although it has been shown atherosclerosis may occur in areas of high WSS [1]. Since the LM, LAD, and LCX have roughly the same diameters, the greater WSS in the LM also suggests the axial fluid velocities in the LM are greater than those in the LAD and LCX. Therefore, it is reasonable to assume that flow velocities play an important role commencement of atherosclerosis and the further study of the velocity field in the coronary arteries is required.

The results showed the magnitude of the WSS near the entrance of the LM was drastically greater than the WSS throughout the majority of the vessel. This elevated WSS near the vessel entrance is somewhat misleading and is the result of flat inlet profile introduced in this study. The WSS in the LM suggest that the flow becomes fully developed, approximately 1.5×10^{-3} m downstream the inlet. The elevated WSS can be alleviated by imposing an inlet profile more indicative of the fully developed profile.

Several studies have demonstrated that formation of atherosclerosis is not likely to occur in regions of the coronary arteries near the inner walls and flow divider of bifurcations [3, 7, 11]. The findings of this work also exhibit this phenomenon, since the WSS is greater near the entrances of the LAD and LCX, than that of the remainder of the vessels. The entrance to these vessels coincides with a bifurcation.

It was apparent from the results, that the magnitude of the WSS was greatest during the times of PFF (ranging from 2.4 Pa to 7.0 Pa) and PA (ranging from 1.5 Pa to 4.0 Pa). This suggests that the development of atherosclerotic lesions is less prevalent during the PFF and PA. In contrast, the lowest WSS were observed during PD (ranging from 0.3 Pa to 2.7 Pa) and PRF (ranging from 0.2 to 1 Pa). This observance leads to the presumption that atheromatous deposits are perhaps more likely to develop and propagate during times of PRF and PD when flow separations and flow reversals occur.

WSS on the upper and lower walls of the LM, LAD and LCX also brings to light important characteristics of the flow in these respective vessels. The WSS of the LCA system implies the following for flow in the vessels: The flow in the LM is symmetric, the flow in the LCX is skewed toward the lower wall near the bifurcation and the flow in the LAD is skewed toward the upper wall near the bifurcation. The stated flow characteristics are consistent with the findings presented by several researchers [7, 17].

ACKNOWLEDGEMENTS

This work was supported in part by the National Institutes of Health (NIH) through Minority Biological Research Support (MBRS) grant, #5O6 6M 0811, through Florida Agricultural and Mechanical University. Sahid C. Smith was supported via a NASA Ph.D. fellowship grant and Shawn Austin through a Title III grant, both through Florida Agricultural and Mechanical University.

TABLE I
Rheological Models

Model	Apparent Viscosity μ, (Pa·s)	Limits on μ in this work
Newtonian	$\mu = \frac{\tau}{\dot{\gamma}}$	None
Power Law	$\mu = m(\dot{\gamma})^{n-1}$ where $m = 0.035$ and $n = 0.6$	when $\dot{\gamma} \geq 327$ $\mu = 0.00345$
Carreau	$\mu = 0.1\left(\mu_\infty + (\mu_0 - \mu_\infty)\left[1+(\lambda\dot{\gamma})^2\right]^{(n-1)/2}\right)$ where $\lambda = 3.313$, $n = 0.3568$, $\mu_0 = 0.56$, and $\mu_\infty = 0.0345$.	None
Walburn-Schneck	$\mu = 0.1\left(C_1 \exp(C_2 H)\exp\left(C_4\left(TPMA/H^2\right)\right)(\dot{\gamma})^{-C_3 H}\right)$ where $C_1 = 0.0797$, $C_2 = 0.0608$, $C_3 = 0.00499$, $C_4 = 14.585$, $H = 40$, and $TPMA = 25.9$	when $\dot{\gamma} \geq 414$ $\mu = 0.00345$
Casson model	$\mu = 0.1\left(\left[\left(\eta^2 J_2\right)^{1/4} + 2^{-1/2}\tau_y^{1/2}\right]^2 J_2^{-1/2}\right)$ where $\lvert\dot{\gamma}\rvert = 2\sqrt{J_2}$, $\tau_y = 0.1(0.625H)^3$, $\eta = \eta_0(1-H)^{-2.5}$	None
Generalized Power Law	$\mu = 0.1\left(\lambda_*\lvert\dot{\gamma}\rvert^{n_*-1}\right)$ $\lambda_*(\dot{\gamma}) = \mu_+ + \Delta\mu \exp\left[-\left(1+\frac{\lvert\dot{\gamma}\rvert}{a}\right)\exp\left(\frac{-b}{\lvert\dot{\gamma}\rvert}\right)\right]$ $n_*(\dot{\gamma}) = n_+ - \Delta n \exp\left[-\left(1+\frac{\lvert\dot{\gamma}\rvert}{c}\right)\exp\left(\frac{-d}{\lvert\dot{\gamma}\rvert}\right)\right]$ where $\mu_+ = 0.035$, $n_+ = 1.0$, $\Delta\mu = 0.25$, $\Delta n = 0.45$, $a = 30$, $b = 3$, $c = 50$, $d = 4$.	None

REFERENCES

1. Fry, D. Acute vascular endothelial changes associated with increased blood velocity gradient. Circulation Research 1968;22: 165-97.

2. Caro, C.G, Fitz-Gerald, J.M., Schroter, R.C. Atheroma and arterial wall shear: observation, correlation and proposal of a shear dependent mass transfer mechanism for atherogenesis. Proceeding of the Royal Society of London 1971;B177: 109-59.

3. Ku, David N., Giddens, Don P., Zarins, Christopher K., Glagov, Seymour. Pulsatile Flow and Atherosclerosis in the Human Carotoid Bifurcation: Positive Correlation between Plaque Location and Low Oscillating Shear Stress. Arteriosclerosis 1985;5: 293-302.

4. Giddens, D.P., Zarins, C.K., Glagov, S. Response of arteries to near wall fluid dynamics behavior. Applied Mechanics Review 1990;43: S98-S102.

5. King, M.J., David, T., Fisher, J. An Initial Parametric Study on Fluid Flow through Bileaflet Mechanical Heart Valves Using Computational Fluid Dynamics. Journal of Engineering in Medicine 1994;208: 63-72.

6. King, M.J., Corden, J., David, T., Fisher, J. A Three- Dimensional, Time-Dependent Analysis of Flow through a Bileaflet Mechanical Heart Valve: Comparison of Experimental and Numerical Results. Journal of Biomechanics 1996;29: 609-18.

7. He, Xiaoyi, Ku, David N. Pulsatile Flow in the Human Left Coronary Artery Bifurcation: Average Conditions. ASME Journal of Biomechanical Engineering 1996;118: 74-82.

8. Shi, Yubing, Zhao, Yong, Yeo, Tony Joon Hock, Hwang, Ned H.C. Numerical Simulation of Opening Process in a Bileaflet Mechanical Heart Valve Under Pulsatile Flow Condition. The Journal of Heart Valve Disease 2003;12: 245-56.

9. Johnston, Barbara M., Johnston, Peter R., Stuart, Corney, Kilpatrick, David. Non- Newtonian blood flow in human right coronary arteries: steady state simulations. Journal of Biomechanics 2004;37: 709-20.

10. Rohlf, K. , Tenti, G. The Role of the Womersley Number in Pulsatile Blood Flow a Theorectical Study of the Casson Model. Journal of Biomechanics 2001;34: 141-8.

11. Asakura, T., Karino, T. Flow patterns and spatial distribution of atherosclerotic lesions in human coronary arteries. Circulation Research 1990;66: 1045-66.

12. Anayiotos, A. 1990. Fluid Dynamics at a Complaint Bifurcation Model. Ph.D. thesis. Georgia Institute of Technology, Atlanta.

13. Moore, James E. Jr., Xu, Chengpei, Glagov, Seymour, Zarins, Christopher K., Ku, David N. Fluid wall shear stress measurements in a model of the human abdominal aorta: oscillatory behavior and relationship to atherosclerosis. Atherosclerosis 1994;110: 225-40.

14. Malek, Adel M., Alper, Seth L., Izumo, Seigo. Hemodynamic Shear Stress and Its Role in Atherosclerosis. Journal of the American Medical Association 1999;282: 2035-42.

15. Chien, Shu, Shunichi, Usami, Taylor, Harry M., Lundberg, John L., Gregersen, Magnus I. Effects of hematocrit amd plamsa proteins on human blood rheology at low shear rates. Journal of Applied Physiology 1966;21: 81-7.

16. Krams, R., Wentzel, J.J, Oomen, J.A.F., Vinke, R., H., J.C., Schuurbiers, de Feyter, P.J., Serruys, P.W., Slager, C.J. Evaluation of endothelial shear stress and 3D geometry as factors determining the develoment of atherosclerosis and remodeling in human coronary arteries in vivo. Arteriosclerosis, Thrombosis and Vascular Biology 1997;17: 2061-5.

17. Perktold, K., Hofer, M., Loew, M., Kuban, B.D., Friedman, M.H. Validated Computation of Physiologic Flow in a Realistic Coronary Artery Branch. Journal of Biomechanics 1998;31: 217-28.